Multidim Syst Sign Process (2010) 21:213–229
DOI 10.1007/s11045-009-0099-y

Perfect histogram matching PCA for face recognition

Ana-Maria Sevcenco · Wu-Sheng Lu

Received: 10 August 2009 / Revised: 21 November 2009 / Accepted: 29 December 2009 /
Published online: 14 January 2010

Abstract We present an enhanced principal component analysis (PCA) algorithm for improving rate of face recognition. The proposed pre-processing method, termed as perfect histogram matching, modifies the image histogram to match a Gaussian shaped tonal distribution in the face images such that spatially the entire set of face images presents similar facial gray-level intensities while the face content in the frequency domain remains mostly unaltered. Computationally inexpensive, the perfect histogram matching algorithm proves to yield superior results when applied as a pre-processing module prior to the conventional PCA algorithm for face recognition. Experimental results are presented to demonstrate effectiveness of the technique.

Keywords Principal component analysis · Histogram matching · Face recognition

1 Introduction

Face recognition has been an active area of research in image processing and computer vision for more than two decades and is certainly one of the most successful applications of contemporary image analysis and understanding. The past two decades have witnessed sustained research endeavors that have led to new methods and algorithms with improved face recognition capability. These include principal component analysis (PCA) (Turk and Pentland 1991; Yang et al. 2004), independent component analysis (ICA) (Bartlett et al. 2002; Kwak and Pedrycz 2007), linear discriminant analysis (LDA) (Etemad and Chellappa 1996), isomaps (Tenenbaum et al. 2000), locally linear embedding (LLE) (Roweis and Saul 2000; Saul and Roweis 2003), Laplacianfaces (He et al. 2005; Niu et al. 2008) based on Laplacian eigenmaps (Belkin and Niyogi 2002, 2008), and whitenedfaces (Liao et al. 2007).

A.-M. Sevcenco · W.-S. Lu (✉)
Department of Electrical and Computer Engineering, University of Victoria,
3800 Finnerty Rd., Victoria, BC V8P 5C2, Canada
e-mail: wslu@ece.uvic.ca

Despite of the emerging nonlinear mapping techniques which preserve the local structure of face images and provide dimensionality reduction (Roweis and Saul 2000; Belkin and Niyogi 2002; Saul and Roweis 2003; Qing and Wang 2006; Niu et al. 2008; Belkin and Niyogi 2008), research interest in PCA-based algorithms for face recognition remains strong. In Ramasubramanian and Venkatesh (2001), a method that combines the discrete cosine transform (DCT), PCA, and the characteristics of the human visual system (HVS) is proposed. In Yang et al. (2004), face images are treated as matrices instead of vectors as in the original PCA algorithm and a corresponding image projection technique is used for face recognition. These methods are shown to offer better recognition rates with improved computational efficiency. In Liao et al. (2007), the authors propose a whitening filter as a pre-processing step, while in Chichizola et al. (2005) a down-sampling step is considered as pre-processing and, in PCA, the eigenfaces are computed directly as the eigenvectors of the covariance matrix. In Hsieh and Tung (2009), an image partition technique is combined with vertically centered PCA and whitened horizontally centered PCA to obtain a novel hybrid approach with better recognition performance relative to the traditional PCA.

Human face recognition is known to be a challenging task, especially because it has to deal with images of a subject with variations in illumination, pose, and expression. Several approaches to tackling the illumination issue in face recognition have been proposed. These include Hallinan (1994) proposing a low-dimensional representation of human faces for arbitrary lighting conditions, Belhumeur et al. (1997) with a post-processing method to accommodate lighting changes, Shashua (1997) with a generalized k-linear reflection model to deal with illumination changes, and some theoretical analysis of illumination in vision systems given by Belhumeur and Kriegman (1996) and Zhao and Yang (1999). Considerable progress in face recognition under pose variations has also been made in the recent years. Li et al. (2000) and Liu and Chen (2003) propose to learn the dynamics of faces from images with continuous pose variation. Recognition-by-synthesis approaches are proposed by Lee and Kim (2004) where a test image with an arbitrary pose is transformed into frontal view, and by Okada and von der Malsburg (2002) where each of the training images is transformed into the same pose as the test image. A probabilistic approach to face recognition is proposed in Kanade and Yamada (2003). In Blanz and Vetter (2003) and Liu and Chen (2005), geometric information of human head are taken into account to aid the recognition.

In this paper, a new pre-processing strategy based on histogram matching is proposed that can be incorporated into the conventional PCA for face recognition. Because of the close connection of the notion of histogram to image's light intensity distribution, to a large extent the method described in this paper is related to the above mentioned work dealing with face images with illumination and facial expression variations, although with a different perspective. Specifically, in Sect. 3 we describe a technique that modifies a given image such that the histogram of the modified image perfectly matches a desirable Gaussian shaped histogram. Through a case study in Sect. 4, it is demonstrated that the perfect histogram matching (PHM) helps generate a considerably more homogeneous tonal distribution in the face images involved in a PCA-based face recognition process so as to improve the recognition rate while the computational complexity required remains low. The experimental results are evaluated by comparing them with those obtained by PCA without pre-processing, and three PCA-based existing algorithms having whitening, discrete cosine transform (DCT) and histogram equalization (HE) pre-processing modules, respectively. For readability and convenience, Sect. 2 presents a brief review of the work of Turk and Pentland (1991); Liao et al. (2007), and Ramasubramanian and Venkatesh (2001) that are most relevant to the work described in this paper.

2 PCA, whitening PCA and DCT-PCA: a review

2.1 PCA

The PCA (Turk and Pentland 1991) is an eigenface-based approach to face recognition that seeks to capture the variation in a collection of face images and uses this information to encode and compare images of individual faces.

The eigenfaces are the eigenvectors of the covariance matrix of the set of face images, where each image is treated as a point in a high dimensional space. Eigenfaces extract relevant facial information, which may or may not be directly related to human intuition of face features such as eyes, nose, and lips, by capturing statistical variation between face images. Therefore, eigenfaces may be considered as a set of features which characterize the global variation among the face images involved. Other advantages of using eigenfaces are an efficient image representation using a small number of parameters and reduced computational and dimensional complexity (Turk and Pentland 1991; Zhao et al. 2003).

Given a data set D, also called training set, consisting of M face images of K individuals, the PCA algorithm proposed in Turk and Pentland (1991) starts by transforming each $N \times N$ image in D into a column vector Γ_i of dimension N^2, by concatenating the image rows. The K individuals involved are called *classes*, each one having $L = M/K$ images in D. Next, an average face Ψ is computed as $\Psi = \frac{1}{M}\sum_{i=1}^{M}\Gamma_i$, and subtracted from each vector Γ_i to construct vector Φ_i as $\Phi_i = \Gamma_i - \Psi$. The data matrix is then formed as $A = [\Phi_1 \ldots \Phi_M]/\sqrt{M}$ and the covariance matrix is constructed as $C = \frac{1}{M}\sum_{i=1}^{M}\Phi_i\Phi_i^T = AA^T$. Note that C is a matrix of large size $N^2 \times N^2$. Instead of directly computing the eigenvectors u_i and eigenvalues λ_i of matrix C, which usually is an intractable task for typical image sizes, the eigenvectors v_i and eigenvalues λ_i of a much reduced size $M \times M$ matrix $L = A^TA$ are computed, and the eigenvectors of matrix C are then found to be

$$u_i = \lambda_i^{-1} A v_i \quad \text{for } i = 1, \ldots, M. \tag{1}$$

These eigenvectors u_i, called eigenfaces, are used to represent the face images from D, so as to examine an input image Γ (in the form of a column vector) as whether or not it is a face image and, if it is, whether or not it is a member of a class or a stranger (non-member).

A p-dimensional face space is generated by the span of the p most significant eigenvectors (i.e. eigenfaces) that are associated with the p largest eigenvalues of C, and the matrix composed of these p eigenfaces is denoted by $\tilde{U}$. Matrix $\tilde{U}$ is used to yield a p-dimensional pattern vector $\Omega = \tilde{U}^T\Phi$ where $\Phi = \Gamma - \Psi$, and is also used to project the input image onto the face space as $\Phi_f = \tilde{U}\tilde{U}^T\Phi = \tilde{U}\Omega$. The Euclidean distance d_0 between the input image Γ and the face space is computed as

$$d_0 = \left\| \Phi - \Phi_f \right\|_2. \tag{2}$$

If distance d_0 is found to be below a chosen threshold δ_0, the input image Γ is classified as a face image, otherwise it is considered a non-face image.

Furthermore, if Γ turns out to be a face image, it can be classified as a class member or non-member face. And if it is a member then the class it belongs is identified. These are achieved by (i) evaluating $d_k = \|\Omega - \Omega_k\|_2$ for $k = 1, \ldots, K$ where the class pattern vector Ω_k is calculated as $\Omega_k = \frac{1}{L}\sum_{i=1}^{L}\Omega_k^{(i)}$ with $\Omega_k^{(i)} = \tilde{U}\Phi_k^{(i)}$ being the pattern vector of the ith image of the kth class; and (ii) comparing

$$d_{\min} = \min_k d_k \tag{3}$$

with a prescribed threshold δ_1. If $d_{\min} = \|\Omega - \Omega_{k^*}\|_2$ and $d_{\min} < \delta_1$, then the input image Γ is identified as a member of class k^*, else Γ is considered a non-member.

2.2 Whitening PCA

As demonstrated by Liao et al. (2007), a pre-processing step of whitening and low-pass filtering that flattens the power spectrum of face images and controls the noise at high frequencies, can improve rate of face recognition. The PCA method with this pre-processing step is called *whitenedfaces* recognition.

The motivation behind whitening technique resides in the spectral behavior of natural scenes and facial images: their power spectra roughly fall with the increasing spatial frequency according to a power law $1/f^{\alpha}$. This unbalanced power spectra may result in potential problems when used in searching for structural information in an image space, as the information at low frequencies may swamp the equally useful information at high frequencies (Liao et al. 2007). The solution in Liao et al. (2007) is to employ a whitening filter to attenuate the low frequencies and boost the high frequencies so as to yield a roughly flat power spectrum across all spatial frequencies, and a low-pass filter to control the noise at high frequencies. This filtering component is integrated as a pre-processing step into the conventional PCA/ICA algorithms, and in this paper the whitenedface recognition employing PCA is called WPCA.

In WPCA, a low-pass filter with frequency response

$$L(f) = \exp\left(-(f/f_c)^n\right) \tag{4}$$

is applied in order to avoid increasing the noise amplitude in image, where the parameters are set to $f_c = 0.6 f_{\max}$, $n = 5$ and $f = \sqrt{u^2 + v^2}$ is the absolute spatial frequency. Subsequently, the whitening filter is applied for balancing the power spectrum. Its frequency response has the expression

$$W(f) = f^{\alpha_\omega/2} \tag{5}$$

where the optimal value of whitening parameter α_ω is found to be 2.5. From (4) and (5), the whitening pre-processing is achieved by applying the combined filter as

$$W_L(f) = W(f)L(f). \tag{6}$$

Multiplying the Fourier coefficients $F(u, v)$ of the face image $I(x, y)$ with the combined filter $W_L(f)$, the result in frequency domain is obtained as

$$F_w(u, v) = W(f)L(f)F(u, v). \tag{7}$$

As a last step of the pre-processing module, the whitenedface image $I_w(x, y)$ is computed using the inverse Fourier transform of (7).

2.3 DCT- PCA

Suppose one performs 2-D DCT of the ith face image in data set D. Mimicking the HVS that is known to be more sensitive to the low-frequency components of an image, one keeps only a certain number of low-frequency DCT coefficients and arranges them as a column vector F_i. In this way, a corresponding data set $\hat{D}$ in the frequency is obtained as $\hat{D} = \{F_1, F_2, \ldots, F_M\}$. By treating $\hat{D}$ as a training set just like in the conventional PCA, a PCA-based algorithm can be applied for face recognition purpose. The orthonormal eigenvectors of the corresponding covariance matrix are called *cosine-faces* (Ramasubramanian and Venkatesh 2001).

Because of the removal of the insignificant spectral components (i.e. the high-frequency DCT coefficients), DCT-PCA based algorithms can perform faster recognition with improved accuracy. In Ramasubramanian and Venkatesh (2001) it is observed that a significant improvement in the recognition rate can be obtained if 30 % of DCT coefficients in the low frequency range are employed.

3 Perfect histogram matching PCA

In this section, we propose a new pre-processing method based on histogram matching that can be incorporated into the conventional PCA for face recognition. The purpose of the histogram matching is to obtain a homogeneous tonal distribution for the face images in the data set D as well as for the input image Γ by modifying the histogram of each image involved to match a desired histogram. In this way, the lighting conditions and light intensities across the entire image set tend to be equalized that in turn reduces the lighting-condition related discrepancy between D and Γ, leading to an improved recognition rate.

3.1 Desired histogram

The histogram of a digital image of size $N \times N$ with G gray levels is a discrete function $h(r_k) = n_k$ with $k = 0, 1, \ldots, G-1$, where r_k is the kth gray level and n_k is the number of pixels in the image having gray level r_k. For an 8-bit digital image, for example, $G = 2^8 = 256$ and r_k assumes discrete values $r_k = 0, 1, \ldots, 255$. The relative frequency of a pixel having gray level r_k in the image is equal to $p_r(r_k) = n_k/n$ where $n = N^2$ is the total number of pixels in the image. It follows that $p_r(r_k)$ is merely a normalized version of the histogram, satisfying

$$0 \leq p_r(r_k) \leq 1 \quad \text{and} \quad \sum_{k=0}^{G-1} p_r(r_k) = 1. \tag{8}$$

For this reason $p_r(r_k)$ is often referred to as probability of occurrence of gray level r_k.

Histograms are the basis for numerous spatial-domain processing techniques for image enhancement, compression and segmentation, being straightforward to calculate and allowing efficient hardware implementations for real-time image processing (Gonzalez and Woods 2002). It is well-known that images with fairly dark characteristics or predominantly light tones can be enhanced by histogram equalization (HE). HE produces an image with nearly uniform distribution over the whole intensity scale, i.e. an image with a flat histogram. More generally, image histogram may be modified to match a particular histogram so as to highlight certain gray-level regions of the image (Gonzalez and Woods 2002). On the other hand, however, current methods for histogram matching achieve its goal only approximately, see for example Sect. 4.2 of Gonzalez and Woods (2002) and Sect. 7.3 of Jain (1989).

For a natural, well-balanced and homogeneous appearance across the face images in data set D, the Gaussian function

$$h_d(r) = ae^{-\frac{(r-b)^2}{2c^2}}, \quad r \in [r_0, r_{G-1}] \tag{9}$$

is chosen to be the desired reference histogram, where parameter b is the position of the center of the peak, c controls the width of the bell shape, a is the height of the curve's peak, and $[r_0, r_{G-1}]$ defines the interval where the Gaussian function specifies the desired histogram.

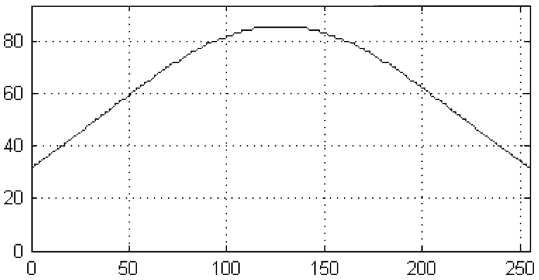

Fig. 1 Gaussian shape of the imposed histogram

Because the gray levels of a digital image always assume integer values and the number of image pixels possessing a given gray level is also an integer, a discrete version of the Gaussian histogram assumes the form

$$h_d(r_k) = \text{round}\left[ae^{-\frac{(r_k-b)2}{2c^2}}\right], \quad \text{for } k = 0, 1, \ldots, G-1 \tag{10}$$

and, for images of size $N \times N$, $h_d(r_k)$ must satisfy the constraint

$$\sum_{k=0}^{G-1} \text{round}\left[ae^{-\frac{(r_k-b)^2}{2c^2}}\right] = N^2 \tag{11}$$

meaning that the total number of pixels in an image with the desired histogram remains to be N^2. For example, for an 8-bit image of size 128×128, we have $N = 128$, $G = 256$, $r_0 = 0$, and $r_{255} = 255$. For a smooth tonal distribution of gray levels, one needs to set the values of parameters b and c such that to provide midtones (Busch 2005; Langford and Bilissi 2005) and a high image contrast (Busch 2005), respectively. Under these circumstances, the left side of (11) becomes a function of one single variable a which can be readily tuned to satisfy (11). For example, for $b = 127.5$, $c = 100$ and $N = 128$ (see Fig. 1), the value of a satisfying (11) is found to be $a = 99.4568$.

3.2 Perfect histogram matching

In what follows, we describe a technique that modifies the histogram of an image to precisely match a desired histogram.

Let the histogram of a digital image Γ of size $N \times N$ be given by $\{h(r_k) = n_k, k = 0, 1, \ldots, G-1\}$ and a desired histogram be given by $\{h_d(r_k) = n_k^{(d)}, k = 0, 1, \ldots, G-1\}$ having the same total number of pixels $n = N^2$ as the original histogram $\{h(r_k)\}$. Viewing the image as a matrix $\Gamma = \{g_{ij}, i, j = 1, 2, \ldots, N\}$, we define index set

$$I_k = \{(i, j) : g_{ij} = r_k\}. \tag{12}$$

Note that (i) the index set I_k contains the pixel locations in the image having gray level r_k; (ii) its length, $|I_k|$, is equal to n_k; and (iii) $\sum_{k=0}^{G-1} |I_k| = N^2 = n$.

With these I_k defined, an ordered index-set sequence I can be constructed as

$$I = \{I_0, I_1, \ldots, I_{G-1}\}. \tag{13}$$

We remark that $I_l \cap I_k = \emptyset$ for $l \neq k$ and $\bigcup_{k=0}^{G-1} I_k$ covers the entire index set $\{(i, j), \quad i, j = 1, 2, \ldots, N\}$. Now if we write index set I explicitly as

$$I = \{(i_1, j_1), (i_2, j_2), \ldots, (i_n, j_n)\}$$

and the desired histogram in terms of a sequence as

$$n^{(d)} = \left\{ n_0^{(d)}, n_1^{(d)}, \ldots, n_{G-1}^{(d)} \right\}$$

which is associated with the gray-level sequence

$$r = \{r_0, r_1, \ldots, r_{G-1}\},$$

then a natural way to modify the gray levels (hence histogram) of the given image to match $n^{(d)}$ is to assign the first gray level r_0 to the first $n_0^{(d)}$ pixels whose locations are specified by the first $n_0^{(d)}$ indices in sequence I. Next, one assigns the second gray level r_1 to the next $n_1^{(d)}$ pixels whose locations are specified by the next $n_1^{(d)}$ indices in I, and so on. The assignment continues until the last gray level r_{G-1} is assigned to the $n_{G-1}^{(d)}$ pixels whose locations are specified by the last $n_{G-1}^{(d)}$ indices in I. From the way the index sequence I is constructed and the histogram of the given image is modified, it follows that (i) the histogram of the given image so modified matches perfectly with the desired histogram; and (ii) subject to perfect histogram matching, the changes made in the histogram of the given image are minimized in the sense that the average difference between the original and modified gray levels at any given pixel location remains smallest.

The implementation of the proposed perfect histogram matching (PHM) pre-processing follows the outline:

Begin: set $index\_length = 0$;
For $k = 0 : 1 : G-1$, do:

- construct the working index set I_w of length $n_k^{(d)}$ as the subset of set I, which consists of the ($index\_length + 1$)th element through the ($index\_length + n_k^{(d)}$)th element in I;
- assign each of the pixels whose locations are specified by I_w to gray level r_k;
- set $index\_length := index\_length + n_k^{(d)}$ and $k := k + 1$;

End

Fig. 2 The effect of PHM pre-processing: original images (*top row*) and their processed counterparts (*bottom row*)

As an example, the PHM algorithm was applied to three facial images of size 128×128 (see the first row of Fig. 2) with $b = 127.5$ and $c = 100$, and the resulting images are shown in the second row of Fig. 2.

For comparison, the effect in spatial and frequency domains of the whitening filter from (6) and the histogram-based processing using (10) is illustrated in Fig. 3 using one of the face images (for display purposes, in this paper, the whitened face image was re-scaled into range [0, 255]).

The method can be summarized by a block diagram in Fig. 4. Central in the system, the PHM module is applied to the training set as well as the test image to obtain a homogeneous tonal distribution. This is followed by the conventional PCA algorithm to yield eigenfaces which are subsequently used to represent and classify the face images. The classification module contains two components: one performs discrimination between face/non-face and member/nom-member images, and the other performs face identification for member images.

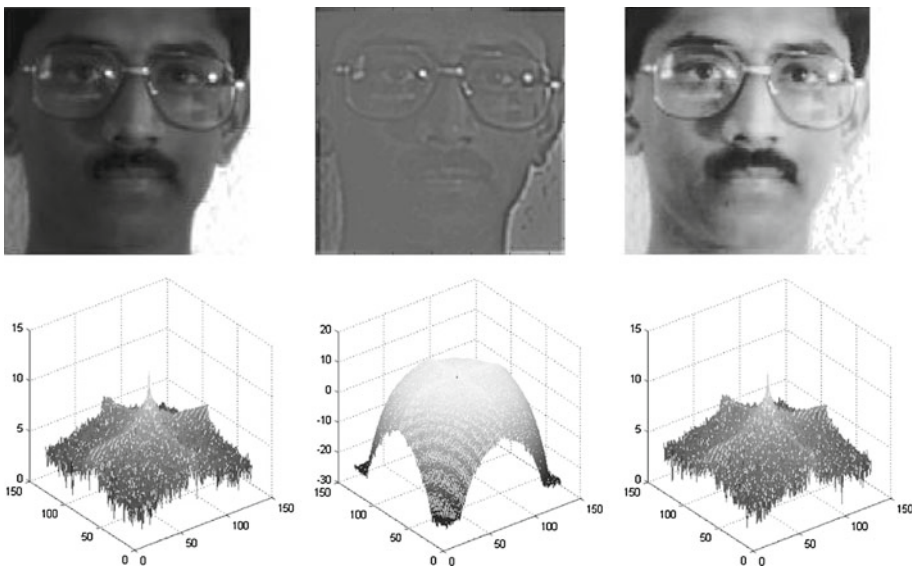

Fig. 3 Top row from left to right: the original face image, its whitened version and its histogram-enhanced version. Bottom row: their corresponding power spectra

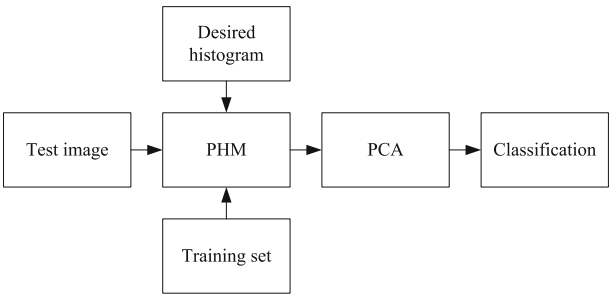

Fig. 4 A block diagram of the proposed method

4 A case study

As a pre-processing algorithm, PHM can in principle be incorporated into any face identification method to enhance its robustness to various facial expressions and illumination-related discrepancy. In this paper, we focus on the case where the PHM algorithm is applied to both the input image Γ and data set D prior to the application of the conventional PCA algorithm. The proposed method will be referred to as the perfect histogram matching PCA (PHM-PCA). Our study aims to evaluate the performance of PHM-PCA and compare it with WPCA (Liao et al. 2007), DCT-PCA (Ramasubramanian and Venkatesh 2001) and PCA (Turk and Pentland 1991) algorithms. The proposed algorithm was also compared with a PCA-based algorithm which incorporates a HE pre-processing step. The Yale Face Database (Belhumeur et al. 1997) and extended Yale Face Database B (Georghiades et al. 2001; Lee et al. 2005) were chosen as image databases as they include more frontal images per class (subject) than several other test data sets (such as FERET) and their images do not need to be rescaled.

The Yale Face Database contains a set of 165 grayscale images of 15 subjects (Fig. 5), with 11 poses per subject (Fig. 6), namely center-light, with glasses, happy, left-light, without glasses, normal, right-light, sad, sleepy, surprised, and wink, denoted as pose 'a', 'b', …, and 'k', respectively. The Yale Face Database images employed in our simulations have been cropped to 128×128 pixel size to minimize non-face areas such as hair and neck, with the image center approximately placed between the 2 nostrils of subject's nose, as illustrated in Figs. 5 and 6.

4.1 Choosing parameters for Gaussian histogram

Throughout the Gausssian histogram in (10) was utilized as the reference histogram where the parameters were set to be $G = 256$, $r_0 = 0$, and $r_{255} = 255$. For a balanced histogram

Fig. 5 The 15 individual members from the data set

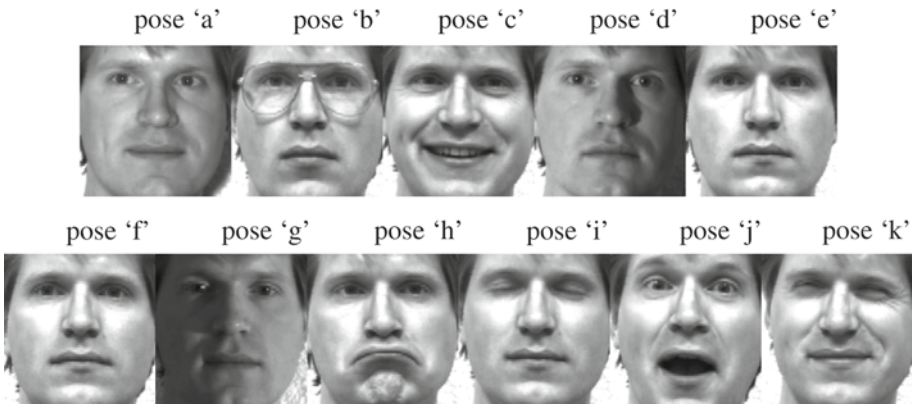

Fig. 6 The 11 poses of one member from the data set

Table 1 Ten cases from Yale Face Database employed for evaluating the performance of PHM-PCA algorithm

	Training set: all 15 members with pose(s)	Testing set: all 15 members with one pose
Case 1	'a', 'c', 'd', 'e', 'g', 'h', 'i'	'f'–normal pose
Case 2	'a', 'd', 'e', 'g'	'f'–normal pose
Case 3	'a', 'e'	'f'–normal pose
Case 4	'a'	'f'–normal pose
Case 5	'a', 'd', 'e', 'g'	'c'–happy pose
Case 6	'a', 'd', 'e', 'g'	'h'–sad pose
Case 7	'a', 'd', 'e', 'g'	'i'–sleepy pose
Case 8	'a', 'd', 'e', 'g'	'j'–surprised pose
Case 9	'a', 'd', 'e', 'g'	'k'–wink pose
Case 10	'a', 'd', 'e', 'g'	'b'–with glasses pose

with midtones, b was set to 127.5. In order to determine the value of c, an exhaustive search was conducted in that the PHM-PCA was applied to a total of ten cases where the training set and testing set varied. As shown in Table 1, these ten cases considered various facial expressions (Cases 1–9), and face obstruction (Case 10). In each case, the training set D consisted of several selected poses of all 15 members while the testing set consisted of all 15 members with one selected pose. For example, in Case 2, D contained a total of $M = 60$ face images involving $k = 15$ members, each with $L = 4$ poses 'a', 'd', 'e', and 'g'; and the testing set contained 15 images from 15 members, each with a normal pose 'f'. In the search, the PHM-PCA was applied to all ten cases with c varying in the range of [1, 1100] and face-space dimension p (see Sect. 2.1) varying in the range of [5, 15]. The value of c that achieved the best overall recognition rate was found to be $c = 100$. The above parameter values were employed throughout our simulations with the Yale Face Database and extended Yale Face Database B.

4.2 Face/non-face and member/non-member discrimination

The training set D used in this case consisted of a total of $M = 48$ images from Yale Face Database with $K = 12$ individuals out of the 15 available subjects from the database, each

Fig. 7 The three non-face images obtained from cropping the original images *airplane*, *boats* and *goldhill*

with $L = 4$ poses, 'a', 'd', 'e' and 'g'. As a result, there were available $M = 48$ eigenfaces from which a subset of $p = 12$ was chosen to represent the face images.

The testing set used to evaluate the discrimination performance of PCA, WPCA, HE-PCA, DCT-PCA and PHM-PCA between face/non-face and member/non-member images consisted of pose 'f' of the 12 individuals from training set, who represented the member images, same pose 'f' of the remaining 3 individuals from the database, who represented the non-member images, labeled as *img8*, *img11* and *img15,* plus 3 non-face images obtained by cropping images *airplane, boats* and *goldhill* to size 128×128 (Fig. 7).

In what follows, we use $C^{(fm)}$ to denote the set of face/member images, and $C^{(nf)}$ and $C^{(nm)}$ to denote the sets of non-face images and non-member images, respectively.

To evaluate the discrimination performance of the five methods, we introduce a measure called $\text{gap}^{(f)}$, which quantifies the distance between the class of non-face images $C^{(nf)}$ and the class of face images $C^{(fm)}$ with respect to face space $\tilde{U}$ (see Sect. 2.1). This measure is defined by

$$\text{gap}^{(f)} = \frac{\min\left(d_0^{(nf)}\right) - \max\left(d_0^{(f)}\right)}{\min\left(d_0^{(nf)}\right)} \cdot 100\ (\%) \tag{14}$$

where $\min(d_0^{(nf)})$ is the smallest d_0 defined by (2) among all non-face images in $C^{(nf)}$, and $\max(d_0^{(f)})$ denotes the largest d_0 among all face images in $C^{(fm)}$.

In addition, a similar measure $\text{gap}^{(m)}$ is defined for quantifying the distance between the class of non-member images $C^{(nm)}$ and the class of member images $C^{(fm)}$ with respect to face space $\tilde{U}$ as

$$\text{gap}^{(m)} = \frac{\min\left(d_{\min}^{(nm)}\right) - \max\left(d_{\min}^{(m)}\right)}{\min\left(d_{\min}^{(nm)}\right)} \cdot 100\ (\%) \tag{15}$$

Table 2 Face/non-face and member/non-member gaps for the mentioned study case from the Yale Face Database

PCA		WPCA		HE-PCA		DCT-PCA		PHM-PCA	
$\text{gap}^{(f)}$	$\text{gap}^{(m)}$	$\text{gap}^{(f)}$	$\text{gap}^{(m)}$	$\text{gap}^{(f)}$	$\text{gap}^{(m)}$	$\text{gap}^{(f)}$	$\text{gap}^{(m)}$	$\text{gap}^{(f)}$	$\text{gap}^{(m)}$
43.09	–	21.42	–	47.96	4.64	43.23	–	50.93	6.91

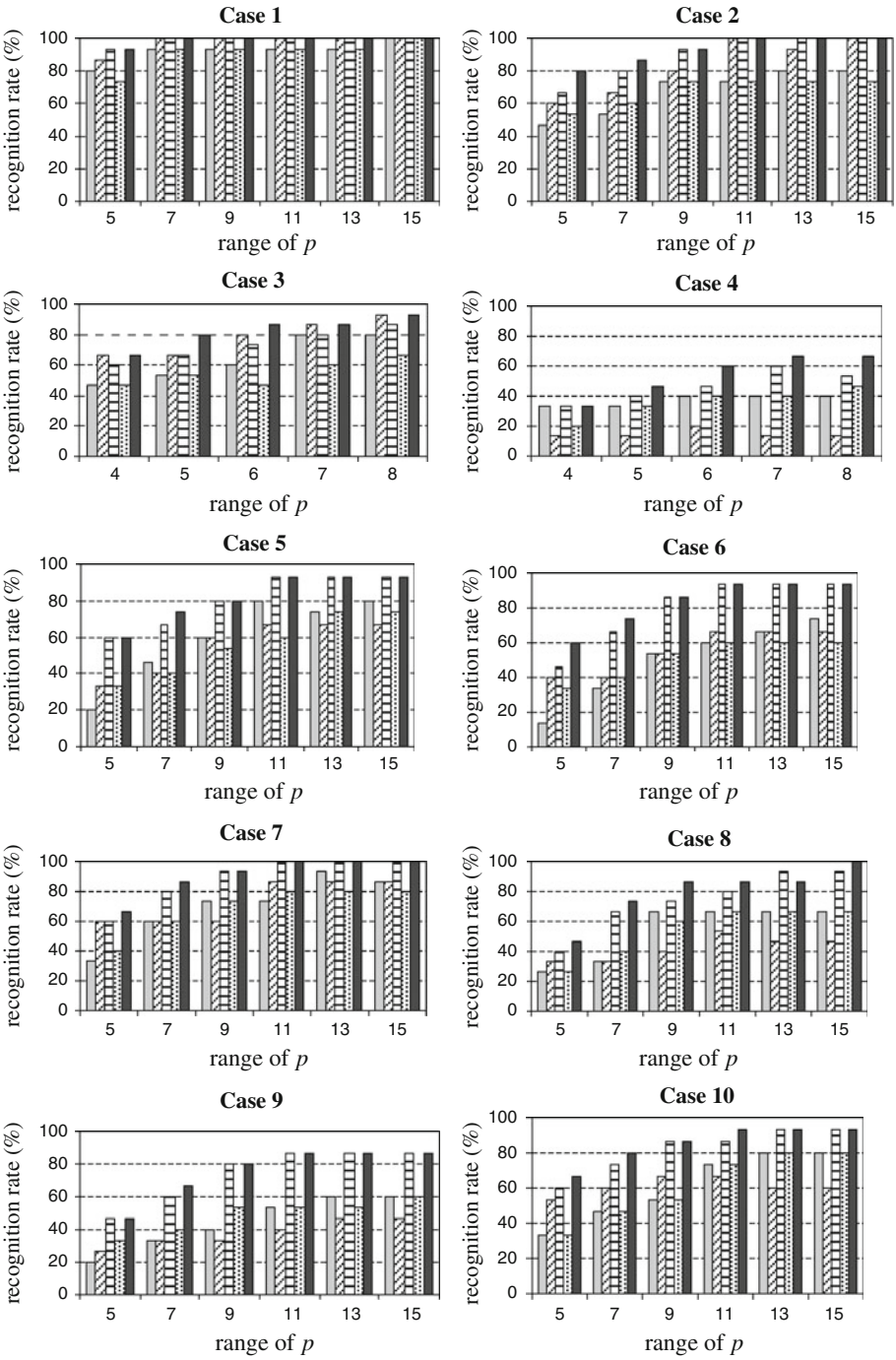

Fig. 8 Comparison results for PCA (*solid grey bar*), WPCA (*diagonal stripped bar*), HE-PCA (*horizontal stripped bar*), DCT-PCA (*dotted bar*) and PHM-PCA (*solid black bar*) using the Yale Face Database

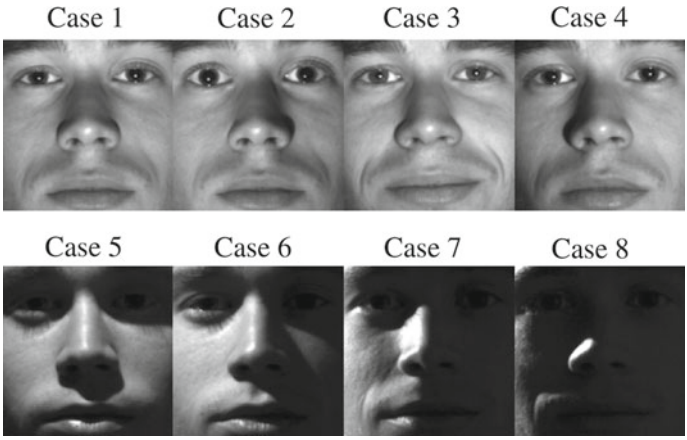

Fig. 9 Eight illumination conditions considered for eight testing sets

where $\min(d_{\min}^{(nm)})$ is the smallest $d_{\min}$ defined by (3) among all non-member images in $C^{(nm)}$, and $\max(d_{\min}^{(m)})$ denotes the largest $d_{\min}$ among all member images in $C^{(fm)}$.

From the definition in (14), it follows that a bigger positive $\text{gap}^{(f)}$ indicates easier face/non-face discrimination, while a negative value of $\text{gap}^{(f)}$ indicates that no discrimination can be made, as the classes $C^{(nf)}$ and $C^{(fm)}$ overlap with each other. A similar claim can be made for member/non-member discrimination based on definition (15). The evaluation results are summarized in Table 2 from which it is observed that PCA and DCT-PCA offered a high gap for face/non-face discrimination, but failed to discriminate members from non-members; WPCA provided only a small gap for face/non-face discrimination and failed in member/non-member discrimination; HE-PCA succeeded in discriminating both cases; and the highest gaps for face/non-face discrimination and member/non-member discrimination was offered by PHM-PCA.

4.3 Face identification

As a first stage of our simulations for face identification, all ten cases in Table 1 were examined. Figure 8 illustrates the comparison results of the five methods in terms of recognition rate versus number (p) of eigenfaces employed. The plots in Fig. 8 show how the recognition rate was improved by utilizing the PHM-PCA algorithm as long as more than 3 eigenvectors were employed for image representation. It is also observed that the performance of PHM-PCA algorithm was quite robust versus the number of images used in the training set. As a matter of fact, even with a reduced training set such as in Cases 3 and 4, the PHM-PCA method outperformed the other four algorithms.

In terms of identification robustness to changes in facial expression (Cases 1–9), Fig. 8 shows that PHM-PCA demonstrated satisfactory performance, with one exception when the training set was very small (Case 4). For slightly obstructed facial images (Case 10), PHM-PCA also offered the best performance among the five algorithms tested.

Face identification under various lighting conditions was also examined in our simulations. For this we employed the extended Yale Face Database B with a selection of 1280 images representing 20 persons with 64 poses per person. Each image was further manually re-cropped to a size of 168×168. The training set contained a total of 400 images repre-

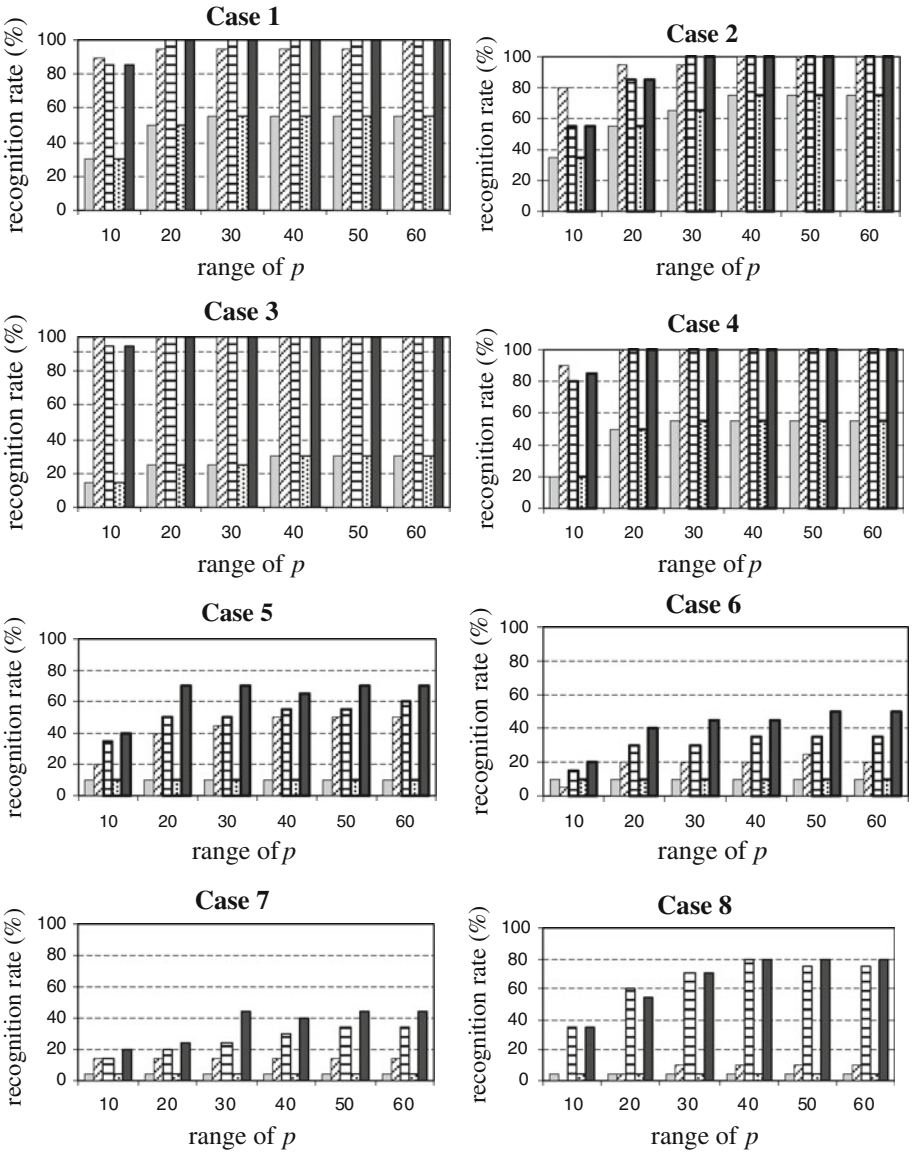

Fig. 10 Comparison results for PCA (*solid grey bar*), WPCA (*diagonal stripped bar*), HE-PCA (*horizontal stripped bar*), DCT-PCA (*dotted bar*) and PHM-PCA (*solid black bar*) using the extended Yale Face Database B

senting 20 individuals with 20 poses per individual. For each individual, eight new poses with various illumination conditions were considered for testing. This yielded eight testing sets, each containing 20 facial images. Figure 9 illustrates as an example eight poses of an individual, each of which belongs to a testing set.

The effect of adopting various number (p) of eigenvalues and lighting conditions on face recognition rate by the five algorithms is illustrated in Fig. 10. It is observed that as long as the lighting condition was such that did not generate large shadowed areas on face (Cases

Table 3 Normalized elapsed time for the five algorithms

PCA	WPCA	HE-PCA	DCT-PCA	PHM-PCA
1	1.32	1.10	0.54	1.12

1–4), PHM-PCA, HE-PCA, and WPCA exhibited comparable and satisfactory performance. Under more extreme lighting conditions (Cases 5–8), PHM-PCA was found to outperform the other four algorithms with one exception in Case 8 with $p = 20$.

Finally, the complexity of the algorithms was examined in terms of normalized elapsed time. Elapsed time rather than the amount of arithmetic computations was chosen as a complexity measure because some of the algorithms under comparison, including HE-PCA and PHM-PCA, involve considerable non-arithmetic operations. Here the elapsed time was normalized so that the "elapsed time" taken by the conventional PCA to perform a face identification task was set to unity.

Table 3 summarizes the average normalized elapsed time over 100 trials of the five algorithms. As expected, DCT-PCA was found to have least complexity. The elapsed time required by PHM-PCA was found slightly higher but comparable with those of HE-PCA and PCA, and less than that of WPCA.

5 Conclusion

The histogram-enhancing method proposed in this paper is conceptually simple, easy to apply, and computationally efficient. It can be used as a pre-processing module in combination with PCA and is shown to be useful for improving the face recognition rate, as demonstrated by the experimental results.

References

Bartlett, M. S., Movellan, J. R., & Sejnowski, T. J. (2002). Face recognition by independent component analysis. *IEEE Transactions on Neural Networks, 13*(6), 1450–1464.

Belhumeur, P. N., Hespanha, J., & Kriegman, D. (1997). Eigenfaces vs. fisherfaces: Recognition using class specific linear projection. *IEEE Transactions on PAMI, Special Issue on Face Recognition, 17*(7), 711–720.

Belhumeur, P., & Kriegman, D. J. (1996). What is the set of images of an object under all possible lighting conditions? In *Proceedings, IEEE conference on CVPR* (pp. 207–277).

Belkin, M., & Niyogi, P. (2002). Laplacian eigenmaps and spectral techniques for embedding and clustering. *Advances in Neural Information Processing Systems, 14*, 585–591.

Belkin, M., & Niyogi, P. (2008). Towards a theoretical foundation for Laplacian-based manifold methods. *Journal of Computer and System Sciences, 74*(8), 1289–1308.

Blanz, B., & Vetter, T. (2003). Face recognition based on fitting a 3D morphable model. *IEEE Transactions on PAMI, 25*(9), 1063–1074.

Busch, D. D. (2005). *Mastering digital SLR photography*. Boston: Thomson Course Technology.

Chichizola, F., De Giusti, L., De Giusti, A., & Naiouf, M. (2005). Face recognition: reduced image eigenfaces method. In *ELMAR 47th International Symposium* (pp. 159–162).

Etemad, K., & Chellappa, R. (1996). Face recognition using discriminant eigenvectors. In *Proceedings, IEEE ICASSP, 4* (pp. 2148–2151).

Georghiades, A. S., Belhumeur, P. N., & Kriegman, D. J. (2001). From few to many: Illumination cone models for face recognition under variable lighting and pose. *IEEE Transactions on PAMI, 23*(6), 643–660.

Gonzalez, R. C., & Woods, R. E. (2002). *Digital image processing* (2nd ed.). New Jersey: Prentice-Hall.

Hallinan, P. (1994). A low-dimensional representation of human faces for arbitrary lighting conditions. In *Proceedings, IEEE CVPR* (pp. 995–999).

He, X., Yan, S., Hu, Y., Niyogi, P., & Zhang, H.-J. (2005). Face recognition using Laplacianfaces. *IEEE Transactions on Pattern Analysis and Machine Intelligence, 27*(3), 328–340.

Hsieh, P.-C., & Tung, P.-C. (2009). A novel hybrid approach based on sub-pattern technique and whitened PCA for face recognition. *Pattern Recognition, 42*(5), 978–984.

Jain, A. K. (1989). *Fundamentals of digital image processing*. New Jersey: Prentice Hall.

Kanade, T., & Yamada, A. (2003). Multi-subregion based probabilistic approach toward pose-invariant face recognition. In *Proceedings, IEEE computational intelligence in robotics automation* (Vol. 2, pp. 954–959) Kobe, Japan.

Kwak, K.-C., & Pedrycz, W. (2007). Face recognition using an enhanced independent component analysis approach. *IEEE Transactions on Neural Networks, 18*(2), 530–541.

Langford, M., & Bilissi, E. (2005). *Langford's advanced photography* (7th ed.). Elsevier: Focal Press.

Lee, H.-S., & Kim, D. (2004). Pose invariant face recognition using linear pose transformation in feature space, In *Proceedings, ECCV workshop computer vision in human-computer interaction*, Czech Republic.

Lee, K. C., Ho, J., & Kriegman, D. (2005). Acquiring linear subspaces for face recognition under variable lighting. *IEEE Transactions on PAMI, 27*(5), 684–698.

Liao, L.-Z., Luo, S.-W., & Tian, M. (2007). "Whitenedfaces" recognition with PCA and ICA. *IEEE Signal Processing Letters, 14*(12), 1008–1011.

Liu, X., & Chen, T. (2003). Video-based face recognition using adaptive hidden Markov models. In *Proceedings, IEEE CVPR, 1* (pp. 340–345).

Liu, X., & Chen, T. (2005). Pose-robust face recognition using geometry assisted probabilistic modeling. In *Proceedings, IEEE CVPR, 1* (pp. 502–509).

Li, Y., Gong, S., & Liddell, H. (2000). Recognizing the dynamics of faces across multiple views. In *Proceedings, British machine vision conference* (pp. 242–251). Bristol, England.

Niu, B., Yang, Q., Shiu, S. C. K., & Pal, S. K. (2008). Two-dimensional Laplacianfaces method for face recognition. *Pattern Recognition, 41*(10), 3237–3243.

Okada, K., & von der Malsburg, C. (2002). Pose-invariant face recognition with parametric linear subspaces. In *Proceedings, 5th international conference on automatic face and gesture recofnition* (pp. 64–69). Washington D.C.

Qing X., & Wang X. (2006). Face recognition using Laplacian+OPRA-faces. *6th World Congress on Intelligent Control and Automation, 2*, 10013–10016.

Ramasubramanian, D., & Venkatesh, Y. V. (2001). Encoding and recognition of faces based on the human visual model and DCT. *Pattern Recognition, 34*(12), 2447–2458.

Roweis, S. T., & Saul, L. K. (2000). Nonlinear dimensionality reduction by locally linear embedding. *Science, 290*(5500), 2323–2326.

Saul, L. K., & Roweis, S. T. (2003). Think globally, fit locally: Unsupervised learning of low dimensional manifolds. *Journal of Machine Learning Research, 4*, 119–155.

Shashua, A. (1997). On photometric issues in 3D visual recognition from a single 2D image. *International Journal of Computer Vision, 21*(1/2), 99–122.

Tenenbaum, J. B., Silva, V., & Langford, J. C. (2000). A global geometric framework for nonlinear dimensionality reduction. *Science, 290*(5500), 2319–2323.

Turk, M. A., & Pentland, A. P. (1991). Face recognition using eigenfaces. In *Proceedings, IEEE computer society conference on computer vision and pattern recognition* (pp. 586–591).

Yale Face Database, CT, USA: Yale University (1997). http://cvc.yale.edu/projects/yalefaces/yalefaces.html.

Yang, J., Zhang, D., Frangi, A. F., & Yang, J.-Y. (2004). Two-dimensional PCA: A new approach to appearance-based face representation and recognition. *IEEE Transactions on Pattern Analysis and Machine Intelligence, 26*(1), 131–137.

Zhao, L., & Yang, Y.-H. (1999). Theoretical analysis of illumination in PCA-based vision systems. *Pattern Recognition, 34*(4), 547–564.

Zhao, W., Chellapa, R., Rosenfeld, A., & Phillips, P. J. (2003). Face recognition: A literature survey. *ACM Computing Surveys*, 399–458.

Author Biographies

Ana-Maria Sevcenco received the engineering degree from Automatic Control and Computer Science Faculty of University of "Politehnica" Bucharest, Romania in 2001, and the M.A.Sc. degree in electrical engineering from the University of Victoria, Victoria, BC, Canada in 2007. Since 2007, she is a Ph.D student in Electrical and Computer Engineering at University of Victoria. Her research interests include digital image processing, face recognition and optimization techniques.

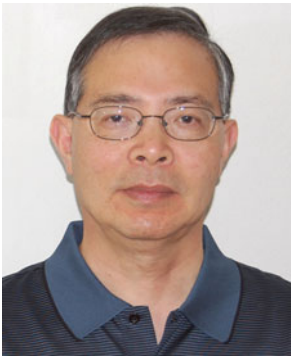

Wu-Sheng Lu received the B.Sc. degree in Mathematics from Fudan University, Shanghai, China, in 1964, and the M.S. degree in Electrical Engineering and the Ph.D. degree in Control Science from the University of Minnesota, Minneapolis, USA, in 1983 and 1984, respectively. He was a post-doctoral fellow at the University of Victoria, Victoria, BC, Canada, in 1985 and a visiting assistant professor with the University of Minnesota in 1986. Since 1987, he has been with the University of Victoria where he is a professor. His current teaching and research interests are in the general areas of digital signal processing and application of optimization methods. He is the co-author with A. Antoniou of Two-Dimensional Digital Filters (Marcel Dekker 1992) and Practical Optimization—Algorithms and Engineering Applications (Springer, 2007). Dr. Lu is a Fellow of Engineering Institute of Canada, and a Fellow of the IEEE.